

# Growth of Cu<sub>2</sub>O/TiO<sub>2</sub> heterojunction and its photoelectrochemical properties

Dengyu Yu, Dengji Yu, Jun Dai, Yunfang Zhang, Fang Wang <sup>\*</sup>

Department of Physics, School of Science, Jiangsu University of Science and Technology, Zhenjiang 212003, China



## ARTICLE INFO

### Article history:

Received 2 November 2019

Received in revised form 2 December 2019

Accepted 21 December 2019

Available online 23 December 2019

### Keywords:

TiO<sub>2</sub> nanoring/nanotube

Cu<sub>2</sub>O

Thermal decomposition

Heterojunction

Photoelectrochemical

## ABSTRACT

In this paper, the Cu<sub>2</sub>O/TiO<sub>2</sub> heterostructure is composed of Cu<sub>2</sub>O particles and TiO<sub>2</sub> nanoring/nanotube (R/T). The high order TiO<sub>2</sub>(R/T) were prepared by two-step anodization. With small diameter Cu<sub>2</sub>O particles deposited on the TiO<sub>2</sub>(R/T) by a simple thermal decomposition process, the photoelectrochemical properties of the TiO<sub>2</sub>(R/T) has been enhanced. As-prepared samples were characterized by scanning electron microscopy, X-ray diffraction and energy dispersive spectrometer. The photoelectrochemical behavior of the samples was studied through electrochemical impedance spectroscopy and photo-to-current conversion efficiency measurement. It was found that the combination of Cu<sub>2</sub>O with TiO<sub>2</sub>(R/T) could not only improve the carrier separation efficiency, but also extend the optical response range of TiO<sub>2</sub>(R/T) to the visible light region. Finally, the mechanism that Cu<sub>2</sub>O can enhance the photoelectrochemical properties of TiO<sub>2</sub>(R/T) is discussed.

© 2019 Elsevier B.V. All rights reserved.

## 1. Introduction

TiO<sub>2</sub> has great potential to solve energy and environmental problems. However, due to its narrow light absorption band and high carrier recombination rate, the use of TiO<sub>2</sub> has been limited [1]. Researchers usually improve its photoelectrochemical properties by modifying or adding captors. Metal doping or noble metal surface modification was usually used for the performance improvement of TiO<sub>2</sub> [2,3]. Recently, experiments have shown that the charge separation efficiency can be improved by heterojunctions formed between TiO<sub>2</sub> NTs and narrow bandgap semiconductors like CdSe, CdS, Bi<sub>2</sub>S<sub>3</sub> and so on [4–6].

The structure of TiO<sub>2</sub> nanotube combined with TiO<sub>2</sub> nanoring has been founded to have better photoelectrochemical properties [7]. It has better light collection cross section and contact area with solution. With the bandwidth of 1.9–2.2 eV and the characteristics of non-toxicity, abundant reserves, low price, Cu<sub>2</sub>O has great potential in the development and utilization of sunlight. However, Cu<sub>2</sub>O photocarriers are unstable and its carriers are very easy to be recombined, which limits its application [8].

Theoretically, Cu<sub>2</sub>O can broaden the absorption spectrum of TiO<sub>2</sub> from the ultraviolet region to the visible region, and the band positions can effectively transfer electrons [9]. However, the size of Cu<sub>2</sub>O particles made by traditional method is so large that it blocks

the pores of TiO<sub>2</sub> NTs, which restrict TiO<sub>2</sub> NTs to exerting its advantages. Recently, a new method of preparing Cu<sub>2</sub>O particles by thermal decomposition can solve it [10].

## 2. Experimental section

### 2.1. Preparation of TiO<sub>2</sub>(R/T) combined structure

TiO<sub>2</sub>(R/T) is obtained from Ti foil by two-step anodic oxidation (see Scheme 1 in [Supporting Information](#)). Anodic oxidation was carried out in a glycol system containing 0.25 wt% NH<sub>4</sub>F and 1.5 vol% deionized water with a two-electrode system. After the anodizing, the film formed by the primary oxidation was removed and then the second anodic oxidation was carried out. After 2 h, the samples were cleaned by ultrasonic with ethanol and deionized water respectively. Finally, the synthetic TiO<sub>2</sub>(R/T) arrays can be achieved by heating to 450 °C for crystallization.

### 2.2. Synthesis of Cu<sub>2</sub>O-TiO<sub>2</sub> heterojunction

The Cu<sub>2</sub>O-decorated TiO<sub>2</sub>(R/T) arrays can be obtained by thermal decomposition of Cu(Ac)<sub>2</sub>(see Scheme 2 in [Supporting Information](#)) [10]. First, the previously prepared TiO<sub>2</sub>(R/T) was immersed in solution of 1 mmol/L of Cu(Ac)<sub>2</sub> for 1 h, and then the samples were rinsed with deionized water at 45 °C and dried at 70 °C. The next step is to decompose the Cu(Ac)<sub>2</sub> molecules into Cu<sub>2</sub>O with a temperature of 400 °C for 2.5 h.

\* Corresponding author.

E-mail address: [wangfang@just.edu.cn](mailto:wangfang@just.edu.cn) (F. Wang).

### 2.3. Photoelectrochemical measurements

Photoelectrochemical measurements were performed using the typical three-electrode system of an CHI660E electrochemical workstation (see Scheme 3 in [Supporting Information](#)).

### 2.4. Characterization

The morphology and structure of the  $\text{Cu}_2\text{O}-\text{TiO}_2(\text{R/T})$  were observed by SEM (ZEISS, the acceleration voltage was 15 kV). An energy dispersive spectrometer (EDX) fitter to the SEM and the mapping corresponding SEM image areas were applied for elemental analysis. The samples are also characterized by XRD (X-ray diffraction) patterns.

## 3. Results and discussion

### 3.1. General characterization

**Fig. 1a** presents an array of tubular structure under the nanoring. The nanoring thickness is smaller than that of nanotubes (**Fig. 1b**). Each nanoring has a diameter of about 100 nm and a wall thickness of 10 nm.  $\text{TiO}_2$  nanotube diameter was about 40 nm and the length was about 3.2  $\mu\text{m}$ . Since the concentration of  $\text{Cu}(\text{Ac})_2$  solution is relatively low, and most of them were attached to the inner wall of NTs, it is not easy to find  $\text{Cu}_2\text{O}$  particles in **Fig. 1c**. EDX and XRD was used to further characterize the samples [11].

**Fig. 1d** shows the XRD pattern (see Scheme 4 in [Supporting Information](#)). Compared with the pure  $\text{TiO}_2(\text{R/T})$  structure, a small diffraction peak appeared in the  $\text{Cu}_2\text{O}-\text{TiO}_2(\text{R/T})$  at the position of 36.54 diffraction Angle (**Fig. 1d**. Inset image), which indicates that the sample contains  $\text{Cu}_2\text{O}$ .

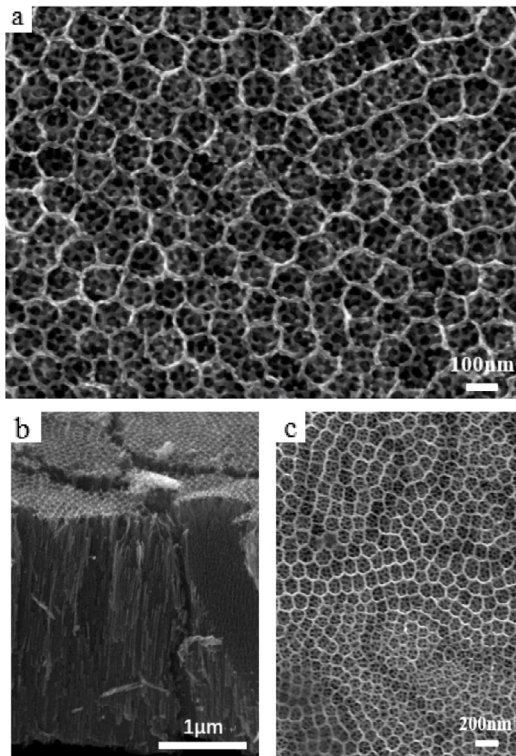


**Fig. 1.** a SEM for  $\text{TiO}_2(\text{R/T})$ . b Cross section view of a. c SEM for  $\text{Cu}_2\text{O}-\text{TiO}_2(\text{R/T})$ . d XRD of  $\text{TiO}_2(\text{R/T})$  (Line 1 A, anatase; T, titanium; C, cuprous oxide) and  $\text{Cu}_2\text{O}-\text{TiO}_2(\text{R/T})$  (Line 2). Insert plot refers to a larger view of the area around C(1 1). e Corresponding EDX spectrum of f. f Top-view SEM of  $\text{Cu}_2\text{O}-\text{TiO}_2(\text{R/T})$ . g Corresponding area element mapping of f (g1 O, g2 Ti, and g3 Cu).

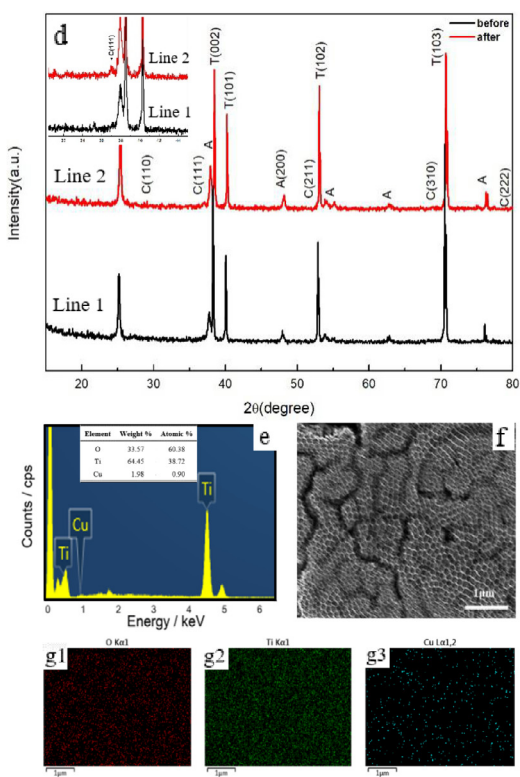
EDX results shows the result after thermal decomposition of 1 mmol/L  $\text{Cu}(\text{Ac})_2$  (**Fig. 1e**). This data further indicates the existence of Cu and it is in agreement with the XRD results. Figure g1, g2 and g3 are mapping of O, Ti and Cu elements respectively, which is consistent with the results in **Fig. 1e**.

### 3.2. Optical property

The IPCE of  $\text{TiO}_2(\text{R/T})$  has two obvious peaks in the wavelength of about 340 nm and 385 nm (**Fig. 2a**). The peak around 385 nm belongs to the  $\text{TiO}_2$  in  $\text{TiO}_2$  nanotube, and the peak around 340 nm belongs to the  $\text{TiO}_2$  nanoring in  $\text{TiO}_2(\text{R/T})$  [12]. After the loading of  $\text{Cu}_2\text{O}$ , The IPCE of the sample is enhanced not only in the range of 300–400 nm, but also in the range of visible light above 400 nm. The peak at wavelength of 375 nm (red line) is still caused by  $\text{TiO}_2(\text{R/T})$  while the enhancement around 300–400 nm is caused by PN junction between  $\text{Cu}_2\text{O}$  and  $\text{TiO}_2(\text{R/T})$  (see [Supporting Information](#)), which can reduce charge recombination. In the visible wavelength part, the enhancement of IPCE mainly comes from the absorption of visible light by  $\text{Cu}_2\text{O}$ .

### 3.3. Photoelectrochemical properties

**Fig. 2b** presents the photocurrent density–time characteristics of  $\text{TiO}_2(\text{R/T})$  and  $\text{Cu}_2\text{O}-\text{TiO}_2(\text{R/T})$ . When turn on the light, the photocurrent of  $\text{TiO}_2(\text{R/T})$  shows a tendency of rapid attenuation from a high current to a low current, while that of  $\text{Cu}_2\text{O}-\text{TiO}_2(\text{R/T})$  shows an upward trend. With the accumulation of time, both of them tend to be stable, and the photocurrent of  $\text{TiO}_2(\text{R/T})$  before and after loading  $\text{Cu}_2\text{O}$  is about 9  $\mu\text{A}/\text{cm}^2$  and 23  $\mu\text{A}/\text{cm}^2$  respectively, which indicates that  $\text{Cu}_2\text{O}$  can effectively improve the photoelectrochemical properties of  $\text{TiO}_2(\text{R/T})$  by reducing the electron-hole recombination. When turn off the light, the dark current of



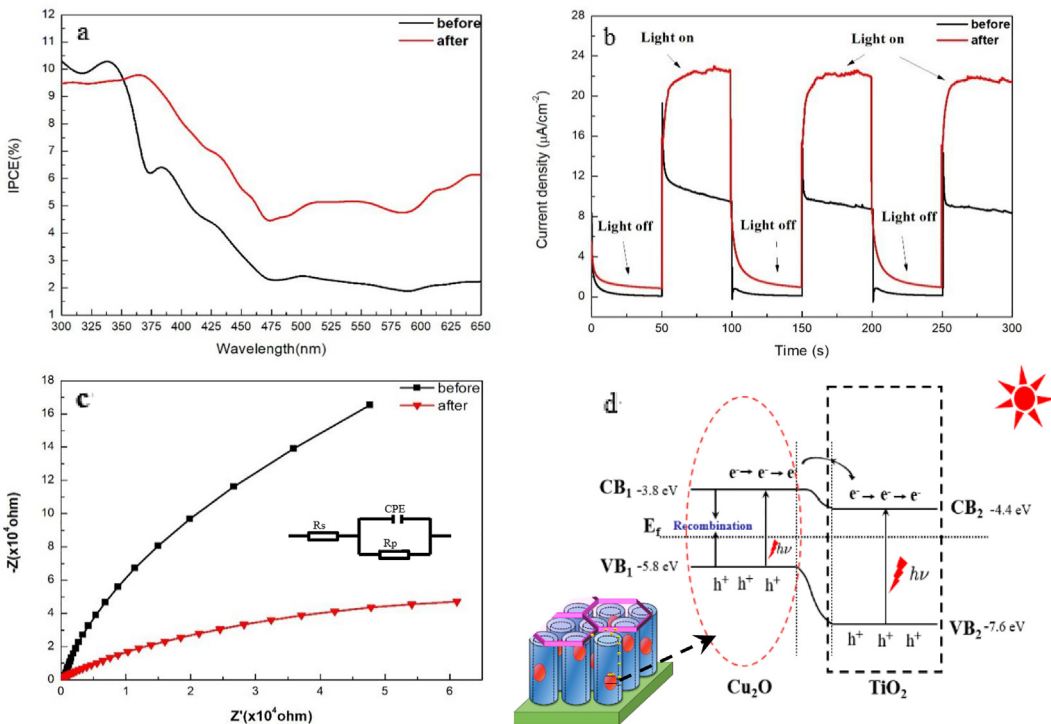


**Fig. 2.** a The IPCE of TiO<sub>2</sub>(R/T) (black) and Cu<sub>2</sub>O-TiO<sub>2</sub>(R/T) (red) respectively. b The photocurrent of TiO<sub>2</sub>(R/T) before and after loading Cu<sub>2</sub>O respectively. c EIS spectra of TiO<sub>2</sub>(R/T) and Cu<sub>2</sub>O-TiO<sub>2</sub>(R/T) respectively. d The photoelectric schematic diagram of Cu<sub>2</sub>O-TiO<sub>2</sub>(R/T).

TiO<sub>2</sub>(R/T) decreases rapidly, while that of Cu<sub>2</sub>O-TiO<sub>2</sub>(R/T) decreases exponentially. This is because, Cu<sub>2</sub>O-TiO<sub>2</sub>(R/T) heterojunction still acts as an obstacle to the electron-hole recombination. In addition, Cu<sub>2</sub>O has a wide band gap which leads to a good response to visible light, so the photocurrent of Cu<sub>2</sub>O-TiO<sub>2</sub>(R/T) can be greatly improved, which is consistent with the result of IPCE.

Fig. 2c is a typical Nyquist plot of TiO<sub>2</sub>(R/T) and Cu<sub>2</sub>O-TiO<sub>2</sub>(R/T). The arc radius of Cu<sub>2</sub>O-TiO<sub>2</sub>(R/T) is significantly less than that of TiO<sub>2</sub>(R/T) and a smaller half arc means faster moving interface charge to electron donors-receptor or photoproduction electron-hole. The inset in Fig. 2c is the equivalent circuit diagram of Cu<sub>2</sub>O-TiO<sub>2</sub>(R/T). R<sub>s</sub> represents the resistance of solution, R<sub>p</sub> represents the resistance of transferring charge from the surface of Cu<sub>2</sub>O-TiO<sub>2</sub>(R/T) to the surface of solution, and CPE represents the constant phase element. Both photocurrent images and EIS spectra reveal that the loading of Cu<sub>2</sub>O can give TiO<sub>2</sub>(R/T) a better photoelectrochemical properties (see Supporting Information).

Fig. 2d shows the charge separation mechanism diagram of Cu<sub>2</sub>O-TiO<sub>2</sub>(R/T) photoanode. The improvement of photochemical properties is attributed not only to visible light, but also to charge separation efficiency. Firstly, Cu<sub>2</sub>O has a good response to visible light because it is a narrow band gap semiconductor and no requirement for momentum condition. Secondly, with the formation of PN junction between Cu<sub>2</sub>O and TiO<sub>2</sub>, a potential barrier is formed between Cu<sub>2</sub>O and TiO<sub>2</sub>. In addition, both the bottom of conduction band and the top of valence band of Cu<sub>2</sub>O is higher than that of TiO<sub>2</sub>. Therefore, photoexcited electrons will directly transfer from the conduction band of Cu<sub>2</sub>O to the conduction band of TiO<sub>2</sub>. Meanwhile, the heterojunction can help these photoexcited electrons to transfer quickly, thus inhibiting carrier recombination [13].

#### 4. Conclusions

In general, we successfully prepared the Cu<sub>2</sub>O-TiO<sub>2</sub>(R/T) heterostructure by means of two-step anodization and thermal

decomposition of Cu(Ac)<sub>2</sub>. XRD, SEM and EDX showed the distribution of Cu<sub>2</sub>O. Photocurrent images showed that the deposition of Cu<sub>2</sub>O can increase the photocurrent of TiO<sub>2</sub>(R/T) effectively. The EIS spectrum reflected the electron action between photoanode and dielectric. IPCE spectrum indicated that Cu<sub>2</sub>O can broaden the optical response range of TiO<sub>2</sub>(R/T) to the visible light region. However, it remains to be studied how much Cu<sub>2</sub>O should be combined on TiO<sub>2</sub>(R/T) and how the length ratio of TiO<sub>2</sub>(R/T) affects the overall heterostructure performance.

#### Declaration of Competing Interest

The authors declare that they have no known competing financial interests or personal relationships that could have appeared to influence the work reported in this paper.

#### Acknowledgements

This work is supported by Jiangsu Province Science Foundation (BK20160561), Foundation of Jiangsu Educational Committee (Grant No.14KJB140004) and National Natural Science Foundation of China (11874185).

#### Author contribution statements

Dengyu Yu and Dengji Yu carried out the experiment. Yunfang Zhang helped supervise the project. Fang Wang and Jun Dai conceived of the original idea. All authors discussed the results and contributed to the final manuscript.

#### Appendix A. Supplementary data

Supplementary data to this article can be found online at <https://doi.org/10.1016/j.matlet.2019.127225>.

## References

- [1] S. Kim, J. Yeo, W. Choi, Simultaneous conversion of dye and hexavalent chromium in visible light-illuminated aqueous solution of polyoxometalate as an electron transfer catalyst, *Appl. Catal. B-Environ.* 84 (2008) 148–155, <https://doi.org/10.1016/j.apcatb.2008.03.012>.
- [2] L.L. Kelly, D.A. Rake, P. Schulz, H. Li, P. Winget, H. Kim, P. Ndione, A.K. Sigdel, J. Brédas, J. Berry, S. Graham, O.L.A. Monti, Spectroscopy and control of near-surface defects in conductive thin film ZnO, *J. Phys.-Condens. Mat.* 28 (2016), <https://doi.org/10.1088/0953-8984/28/9/094007>.
- [3] A. Fujishima, X.T. Zhang, D.A. Tryk., TiO<sub>2</sub> photocatalysis and related surface phenomena, *Surf. Sci. Rep.* 63 (2008) 515–582, <https://doi.org/10.1016/j.surfrep.2008.10.001>.
- [4] A.K. Ayal, Z. Zainal, H.N. Lim, et al., Fabrication of CdSe nanoparticles sensitized TiO<sub>2</sub> nanotube arrays via pulse electrodeposition for photoelectrochemical application, *Mater. Res. Bull.* 106 (2018) 257–262, <https://doi.org/10.1016/j.materresbull.2018.05.040>.
- [5] J. Xie, W. Hong, M. Meng, M. Tian, C. Kang, Z. Zhou, C. Chen, Y. Tang, G. Luo, Synthesis and photocatalytic activity of cerium-modified CdS-TiO<sub>2</sub> photocatalyst for the formaldehyde degradation at room temperature, *Z. Anorg. Allg. Chem.* 644 (2018) 1570–1575, <https://doi.org/10.1002/zaac.201800315>.
- [6] Z.C. Guan, X. Wang, P. Jin, Enhanced photoelectrochemical performances of ZnS-Bi<sub>2</sub>S<sub>3</sub>/TiO<sub>2</sub>/WO<sub>3</sub> composite film for photocathodic protection, *Corros. Sci.* 143 (2018) 31–38, <https://doi.org/10.1016/j.corsci.2018.07.037>.
- [7] F. Wang, Y. Liu, W. Dong, M.R. Shen, Z.H. Kang, Tuning TiO<sub>2</sub> photoelectrochemical properties by nanoring/nanotube combined structure, *J. Phys. Chem. C* 115 (2011) 14635–14640, <https://doi.org/10.1021/jp203665j>.
- [8] P.E. de Jongh, D. Vanmaekelbergh, J.J. Kelly, Cu<sub>2</sub>O: electrodeposition and characterization, *Chem. Mater.* 11 (1999) 3512–3517, <https://doi.org/10.1021/cm991054e>.
- [9] W. Zhu, B.H. Chong, K. Qin, L. Guan, X. Hou, G.Z. Chen, Cuprous oxide/titanium dioxide nanotube-array with coaxial heterogeneous structure synthesized by multiple-cycle chemical adsorption plus reduction method, *RSC Adv.* 6 (2016) 59160–59168, <https://doi.org/10.1039/C6RA06893F>.
- [10] Y. Liao, P. Deng, X. Wang, D. Zhang, F. Li, Q. Yang, H. Zhang, Z. Zhong, A facile method for preparation of Cu<sub>2</sub>O-TiO<sub>2</sub> NTA heterojunction with visible-light photocatalytic activity, *NRL* 13 (2018) 221, <https://doi.org/10.1186/s11671-018-2637-8>.
- [11] Y. Li, Y. Wang, J. Kong, H. Jia, Z. Wang, Synthesis and characterization of carbon modified TiO<sub>2</sub> nanotube and photocatalytic activity on methylene blue under sunlight, *Appl. Surf. Sci.* 344 (2015) 176–180, <https://doi.org/10.1016/j.apsusc.2015.03.085>.
- [12] J. Xue, Q. Shen, W. Liang, X. Liu, B. Xu, Controlled synthesis of coaxial core-shell TiO<sub>2</sub> /Cu<sub>2</sub>O heterostructures by electrochemical method and their photoelectrochemical properties, *Mater. Lett.* 92 (2013) 239–242, <https://doi.org/10.1016/j.matlet.2012.10.127>.
- [13] L.Y. Xiang, J. Ya, F.J. Hu, L.X. Li, Z.F. Liu, Fabrication of Cu<sub>2</sub>O/TiO<sub>2</sub> nanotube arrays with enhanced visible-light photoelectron catalytic activity, *Appl. Phys. A* 123 (2017) 160, <https://doi.org/10.1007/s00339-017-0799-3>.